Volume 43 | Number 31 | 21 August 2014 | Pages 11769–12110

Dalton Transactions

An international journal of inorganic chemistry

www.rsc.org/dalton

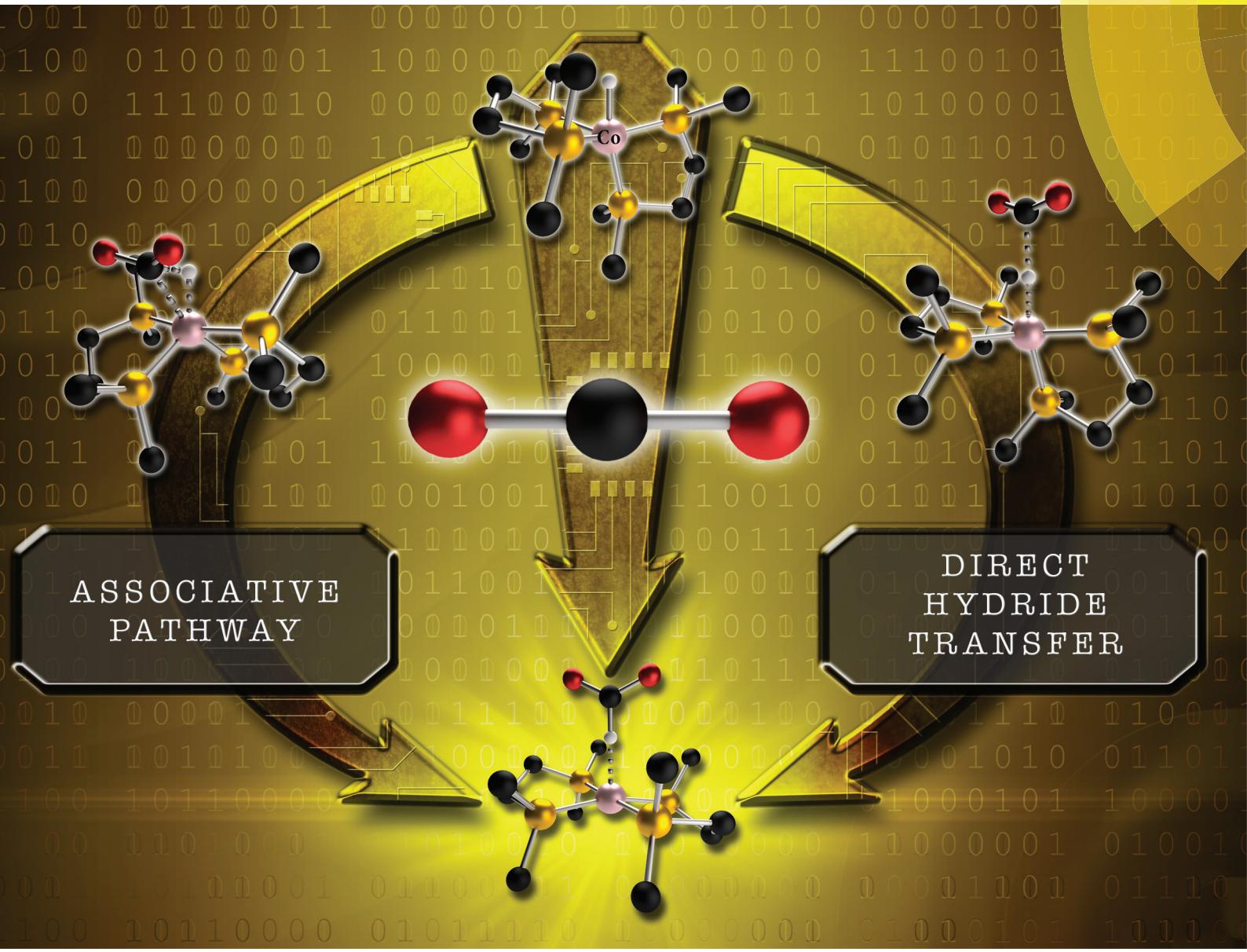

ISSN 1477-9226

ROYAL SOCIETY OF CHEMISTRY

COMMUNICATION

S. Raugei, A. M. Appel *et al.*

Mechanistic insights into hydride transfer for catalytic hydrogenation of CO_2 with cobalt complexes

Dalton Transactions

COMMUNICATION

View Article Online
View Journal | View Issue

Cite this: *Dalton Trans.*, 2014, **43**, 11803

Received 27th May 2014,
Accepted 11th June 2014

DOI: 10.1039/c4dt01551g

www.rsc.org/dalton

Mechanistic insights into hydride transfer for catalytic hydrogenation of CO_2 with cobalt complexes†

N. Kumar, D. M. Camaioni, M. Dupuis, S. Raugei* and A. M. Appel*

The catalytic hydrogenation of CO_2 to formate by $Co(dmpe)_2H$ can proceed *via* direct hydride transfer or *via* CO_2 coordination to Co followed by reductive elimination of formate. The different nature of the rate-determining step in the two mechanisms may provide new insights into designing catalysts with improved performance.

Increasing the use of carbon-neutral energy sources, such as solar and wind, will be facilitated by the ability to design catalysts for the interconversion of electrical and chemical energy. Such catalysts could be used to convert carbon-neutral electricity to fuels, or transform gaseous fuels, such as H_2, into carbon-based liquid fuels through the hydrogenation of CO_2. The development of a synthetic carbon cycle based on carbon-neutral energy would have the potential for large-scale expansion in the use of renewable energy for transportation.[1] However, the rational design of stable, highly active, and energy efficient catalysts for this transformation has remained elusive.

Frequently, the first step in the hydrogenation of CO_2 using molecular catalysts yields formic acid (HCO_2H) or formate (HCO_2^-). Molecular catalysts have been reported in the literature for the conversion of CO_2 to formate, however, many of them are based on expensive metals such as Ir,[1c,2] Ru,[3] and Rh,[4] and typically they operate at high temperature and/or pressure. Recently, our group has developed a first row transition metal catalyst for hydrogenation of CO_2 to formate,[5] a cobalt-hydride bis-diphosphine complex $Co(dmpe)_2H$ (dmpe is 1,2-bis(dimethylphosphino)-ethane). The catalytic cycle is proposed to involve three steps (Fig. 1). The first step is postulated to be rate determining and consists of an overall hydride transfer to CO_2 to form $[Co(dmpe)_2]^+$ and formate. However, the precise mechanism by which this step occurs has not been elucidated. The next two steps in the catalytic cycle are the addition of H_2 to form a Co(III) dihydride followed by the deprotonation of the dihydride by an external base to regenerate the Co(I) hydride. In this study, we seek a detailed characterization of the hydride transfer step with the goal of determining the factors limiting catalysis.

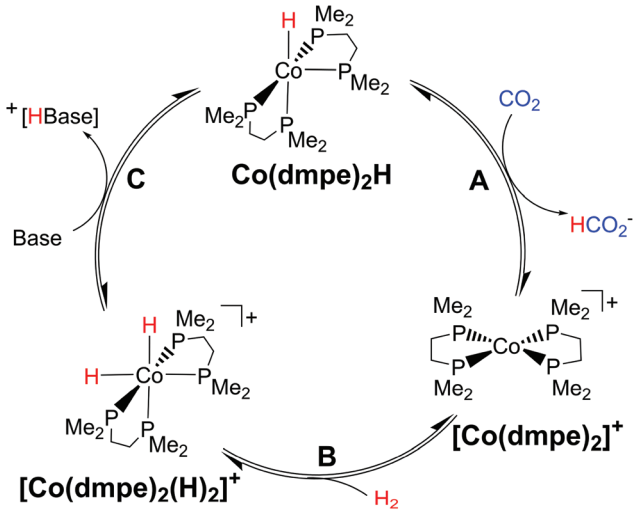

Fig. 1 Proposed catalytic cycle for the hydrogenation of CO_2.

Two possible routes are investigated for the transfer of a hydride from $Co(dmpe)_2H$ to CO_2, as shown in Fig. 2: (I) a *direct hydride transfer* that involves transfer of the hydride directly from the metal complex to an encountered CO_2; (II) an *associative* pathway, which involves binding of CO_2 through its carbon to the metal[6] (resulting in a formal oxidation to Co(III)) followed by reductive elimination to generate formate and the Co(I) complex. The possibility of the *associative* pathway was considered because the $Co(dmpe)_2H$ complex is five-coordinate, and we hypothesized that the Co center could participate in the CO_2 activation.

To characterize the key species involved in these two pathways, quantum mechanical calculations were carried out using the hybrid B3P86[7] exchange and correlation functional and 6-31G** basis set for all the non-metal atoms and the

Pacific Northwest National Laboratory, P.O. Box 999, MS K2-57, Richland, WA 99352, USA. E-mail: simone.raugei@pnnl.gov, aaron.appel@pnnl.gov; Tel: +1-509-372-6902+1-509-375-2157

†Electronic supplementary information (ESI) available: Details of the computational methods, NBO analysis, optimized geometries (in THF and MeCN) and *XYZ* coordinates of the all the species. See DOI: 10.1039/c4dt01551g

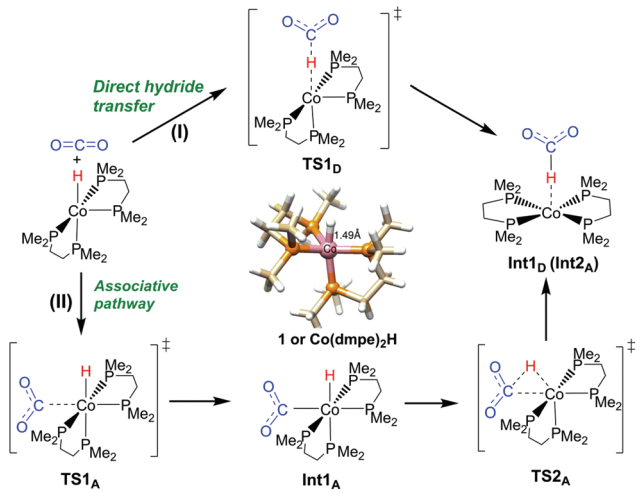

Fig. 2 Possible routes studied for hydride transfer from Co–H to CO_2.

Stuttgart–Dresden relativistic effective core potential and its associated basis set (SDD)[8] for Co. This level of theory has been shown to provide good accuracy for the prediction of the thermodynamics properties (hydricities, acidities, and reduction potentials) and reactivity of cobalt and nickel hydride complexes.[9] For $HCo(dmpe)_2$ the thermodynamic data were determined in acetonitrile (MeCN) solution,[5,9b,10] whereas catalysis for the hydrogenation of CO_2 was investigated in tetrahydrofuran (THF).[5] Accordingly, calculations were performed in both solvents (for more details, see ESI†).

The free energy profile for the *direct transfer* of the hydridic hydrogen to CO_2 without binding of the CO_2 to the metal center is displayed in Fig. 3 (optimized structures of relevant stationary points are illustrated in Fig. S1 and S2†). The reaction involves a weakly bound intermediate RC_D resulting from

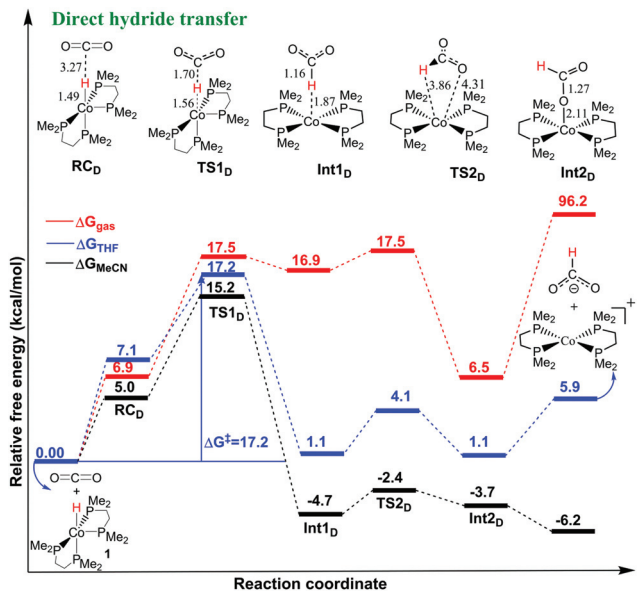

Fig. 3 Free energy profile of *direct hydride transfer* pathway relative to the total energy of $Co(dmpe)_2H$ and CO_2.

electrostatic interactions between the electrophilic carbon of CO_2 and the Co–H moiety. However, the loss of entropy make the formation of RC_D endergonic (+7.1 kcal mol^{-1} in THF, and +5.0 in MeCN). RC_D is considered to be the initial catalytic state in the activation of CO_2 and it shows an OCO bond angle of (178.8°) that is close to free CO_2. The free energy of activation for the hydride transfer $TS1_D$ (relative to unbound $Co(dmpe)_2H$ and CO_2) is calculated to be a 17.2 kcal mol^{-1} in THF. The $TS1_D$ possesses an imaginary vibrational frequency of $411i$ cm^{-1} corresponding to the movement of the hydride along the axis containing carbon of the CO_2, and cobalt metal. The key entities (carbon, hydride and Co atoms) are strictly confined to a linear conformation and both bonds (Co–H = 1.56 Å and C–H = 1.70 Å in THF) are stretched along the reaction coordinates whereas the OCO bond angle is reduced significantly to 153° (see Fig. S1†). The nucleophilic attack of the hydride to CO_2 leads to the formation of a H-bound formate $Int1_D$ complex (OCO angle of 129.5°, consistent with a formate ion), strongly hydrogen bonded to the metal center (see Natural Bond Orbital analysis in ESI and Fig. S3†). The hydride transfer reaction is slightly endergonic in THF (+1.1 kcal mol^{-1}) and exergonic in MeCN (−4.7 kcal mol^{-1}) relative to the energy of CO_2 and $Co(dmpe)_2H$.

The intermediate $Int1_D$ complex can undergo a facile intramolecular rearrangement *via* a transition state $TS2_D$ (activation barrier of only 3.0 kcal mol^{-1} relative to $Int1_D$ in THF) to form an O-bound (Co–(η^1-OCOH)) formate complex (Fig. S1 and S2†). The relative free energies of both intermediates ($Int1_D$ and $Int2_D$) are similar, +1.1 and +1.1 kcal mol^{-1} in THF. Due to the similarities in energies as well as the low barrier for their interconversion, formate could be released from either of these intermediates.

Similar pathways with distinct elementary steps for hydride transfer and the subsequent rearrangement from an H-bound to O-bound formate have been suggested previously for the Ir[6b,11] and Ru[6d] metal complexes. In particular, the formation of O-bound formate intermediate with *trans*-$[Ru(dmpe)_2H_2]$ complex was also reported in previous studies.[6d] However, in these cases, the hydride transfer step was not the rate determining step.[6c,12] In contrast, in the present work, the *direct hydride transfer* pathway is clearly limited by the hydride transfer step, and not by the subsequent rearrangement.

The calculated overall free energy required for the hydrogenation of CO_2 to formate is −6.2 kcal mol^{-1} (Fig. 3) in MeCN, which compares favorably with previous estimated values of −8 kcal mol^{-1}.[5,9b,10] Instead, the reaction in THF was calculated to be uphill by 5.9 kcal mol^{-1}. This difference in overall free energy indicates a large solvent effect, consistent with the different dielectric constants of the two solvents and consequently their different ability to solvate the formate anion.

For further comparison, we explored an *associative* pathway in which CO_2 binds to the metal center rather than interacting directly with the hydridic hydrogen as in the *direct hydride transfer* pathway. The reaction free energy profile is shown in Fig. 4 (optimized structures are given in Fig. S4 and S5†). The

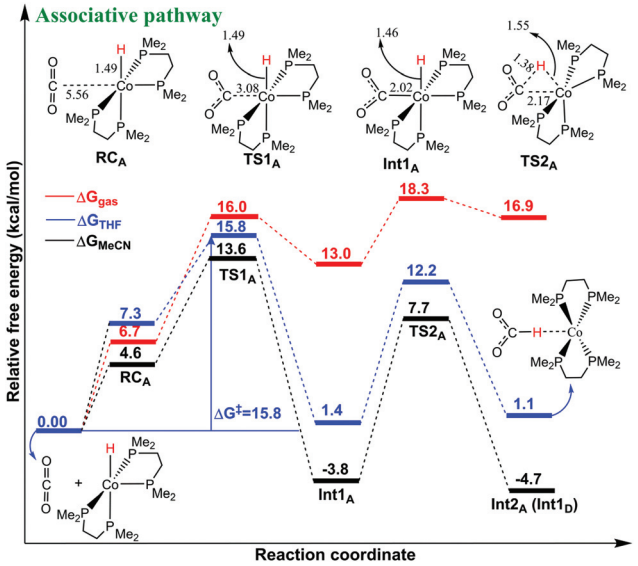

Fig. 4 Free energy profile of *associative* pathway relative to the total energy of $Co(dmpe)_2H$ and CO_2.

initial step in the *associative* pathway is the binding of CO_2 to the Co metal center with the endergonic formation of the encounter complex RC_A, which has an association free energy of +7.3 kcal mol^{-1} and a Co···CO_2 distance of 5.56 Å in THF solution. In spite of the notable structural difference between RC_D (from the *direct hydride transfer* pathway) and RC_A, there is only a small energetic difference (0.2 kcal mol^{-1} in THF) between the two structures. The association of CO_2 proceeds by binding CO_2 to the Co to form a six coordinated $Co(dmpe)_2(H)(CO_2)$ precursor complex $Int1_A$ *via* the transition state $TS1_A$ (with activation barrier of +15.8 kcal mol^{-1} and +13.6 kcal mol^{-1} in THF and MeCN, respectively). This coordination results in a change of formal oxidation state of the metal center from Co(I) to Co(III). $TS1_A$ is characterized by an OCO bond angle of 158°, a Co–C distance of 3.08 Å, and an imaginary frequency of 154*i* cm^{-1} (Fig. S4†). The formation of the pseudo octahedral intermediate $Int1_A$ is mildly endergonic in THF (+1.4 kcal mol^{-1} relative to $Co(dmpe)_2H$ and CO_2) and appreciably exergonic in MeCN (−3.8 kcal mol^{-1}). From the NBO analysis (Table S2†), the total charge on the CO_2 group in CO_2-bound six-coordinate intermediate $Int1_A$ is calculated to be −0.64, indicating that the CO_2 is activated. Subsequently, the intermediate $Int1_A$ undergoes an intramolecular hydride transfer from the Co center to the electrophilic carbon of CO_2. This step generates the H-bound intermediate formate complex $Int2_A$ *via* a triangle-shaped transition state $TS2_A$ (+12.2 kcal mol^{-1} and +7.7 kcal mol^{-1} in THF and MeCN, respectively, with an imaginary frequency of 271*i* cm^{-1}). In $TS2_A$, the Co–H and Co–C bonds are elongated to 1.55 Å and 2.17 Å respectively, whereas C–H distance is reduced to 1.38 Å (see Fig. S4†). This reductive elimination step yields $Int2_A$, which has a molecular structure and relative energy similar to the intermediate $Int1_D$ that is formed in the *direct hydride transfer* pathway. Therefore, the H-bound formate complex is generated in either pathway and can rearrange to the O-bound formate complex and dissociate.

Binding of CO_2 to form the six-coordinate Int_{1A} complex has the highest activation barrier in the *associative pathway*. In contrast, the highest barrier found in the *direct hydride transfer* mechanism comes from the hydride transfer (confirmed with frontier molecular orbitals diagram in Fig. S6†). The barrier for the *associative pathway* is slightly lower (~1.4 kcal mol^{-1}) than for the *direct hydride transfer* pathway in both THF and MeCN (Table S1†). Note that different DFT exchange and correlation functionals and basis sets (see discussion in ESI†) give similar results. Therefore, the present calculations favor the reduction of CO_2 by $Co(dmpe)_2H$ as occurring by an associative pathway with CO_2 binding to the metal center, followed by a reductive elimination. However, because the barriers for the two calculated pathways are very close in energy, the *direct hydride transfer* mechanism is also possible. In addition, the calculated barriers for both mechanisms (17.2 kcal mol^{-1} and 15.8 kcal mol^{-1}) are consistent with the experimentally observed rate (turnover frequency of 3400 h^{-1} at 21 °C in THF) that corresponds to an overall barrier of 17.5 kcal mol^{-1} through transition state theory.

As a possible approach to distinguishing between the *direct hydride transfer* and *associative* mechanisms, we calculated the kinetic isotope effects (KIE). The KIE values were determined from the vibrational frequency calculations that include the zero point energy (ZPE) terms by labeling hydride with deuterium. Due to the very different nature of the rate determining steps, the two mechanisms displayed distinct KIE values (Table S1†). The *direct hydride transfer* pathway shows a normal KIE (K_H/K_D = 1.33) consistent with the hydride transfer being the rate-limiting step. In contrast, the *associative pathway* is characterized by a small inverse isotope effect (K_H/K_D = 0.92), which is consistent with the fact that the hydride transfer is not the rate-determining step in the *associative pathway*. The two pathways may be experimentally distinguishable based on the difference in the KIEs.

In summary, the present computational study suggests two possible pathways for the catalytic hydrogenation of CO_2 using $Co(dmpe)_2H$ complex. The *associative* pathway, in which CO_2 binds to the metal center first, is favored by approximately 1.4 kcal mol^{-1} over the *direct hydride transfer* pathway in which the hydride is directly transferred from the cobalt complex to CO_2. To the best of our knowledge, the pre-coordination of CO_2 to Co as a rate-determining step in the *associative pathway* has not been reported before for M–H complexes. The accessibility of this new pathway may provide valuable insight for the rational design of catalysts.

Acknowledgements

The authors thank Dr Jonathan M. Darmon for the preparation of the Cover Artwork. The research by N.K., D.M.C. and A.M.A. was supported by the US Department of Energy, Office of Basic Energy Sciences, Division of Chemical Sciences, Geosciences &

Biosciences. The research by S.R. and M.D. was supported as part of the Center for Molecular Electrocatalysis, an Energy Frontier Research Center funded by the U.S. Department of Energy, Office of Science. Pacific Northwest National Laboratory (PNNL) is a multiprogram national laboratory operated for the DOE by Battelle.

Notes and references

1 (*a*) T. R. Cook, D. K. Dogutan, S. Y. Reece, Y. Surendranath, T. S. Teets and D. G. Nocera, *Chem. Rev.*, 2010, **110**, 6474–6502; (*b*) G. A. Olah, G. K. S. Prakash and A. Goeppert, *J. Am. Chem. Soc.*, 2011, **133**, 12881–12898; (*c*) J. F. Hull, Y. Himeda, W.-H. Wang, B. Hashiguchi, R. Periana, D. J. Szalda, J. T. Muckerman and E. Fujita, *Nat. Chem.*, 2012, **4**, 383–388; (*d*) A. M. Appel, J. E. Bercaw, A. B. Bocarsly, H. Dobbek, D. L. DuBois, M. Dupuis, J. G. Ferry, E. Fujita, R. Hille, P. J. A. Kenis, C. A. Kerfeld, R. H. Morris, C. H. F. Peden, A. R. Portis, S. W. Ragsdale, T. B. Rauchfuss, J. N. H. Reek, L. C. Seefeldt, R. K. Thauer and G. L. Waldrop, *Chem. Rev.*, 2013, **113**, 6621–6658; (*e*) C. Ziebart, C. Federsel, P. Anbarasan, R. Jackstell, W. Baumann, A. Spannenberg and M. Beller, *J. Am. Chem. Soc.*, 2012, **134**, 20701–20704; (*f*) R. Langer, Y. Diskin-Posner, G. Leitus, L. J. W. Shimon, Y. Ben-David and D. Milstein, *Angew. Chem., Int. Ed.*, 2011, **50**, 9948–9952.

2 T. J. Schmeier, G. E. Dobereiner, R. H. Crabtree and N. Hazari, *J. Am. Chem. Soc.*, 2011, **133**, 9274–9277.

3 (*a*) P. G. Jessop, T. Ikariya and R. Noyori, *Chem. Rev.*, 1995, **95**, 259–272; (*b*) P. G. Jessop, F. Joo and C.-C. Tai, *Coord. Chem. Rev.*, 2004, **248**, 2425–2442.

4 J. C. Tsai and K. M. Nicholas, *J. Am. Chem. Soc.*, 1992, **114**, 5117.

5 M. S. Jeletic, M. T. Mock, A. M. Appel and J. C. Linehan, *J. Am. Chem. Soc.*, 2013, **135**, 11533–11536.

6 (*a*) F. Hutschka, A. Dedieu, M. Eichberger, R. Fornika and W. Leitner, *J. Am. Chem. Soc.*, 1997, **119**, 4432–4443; (*b*) W. H. Bernskoetter and N. Hazari, *Eur. J. Inorg. Chem.*, 2013, **2013**, 4032–4041; (*c*) Y.-Y. Ohnishi, Y. Nakao, H. Sato and S. Sakaki, *Organometallics*, 2006, **25**, 3352; (*d*) Y.-Y. Ohnishi, T. Matsunaga, Y. Nakao, H. Sato and S. Sakaki, *J. Am. Chem. Soc.*, 2005, **127**, 4021.

7 (*a*) J. P. Perdew, *Phys. Rev. B: Condens. Matter*, 1986, **33**, 8822; (*b*) A. D. Becke, *J. Chem. Phys.*, 1993, **98**, 5648–5652.

8 D. Andrae, U. Häußermann, M. Dolg, H. Stoll and H. Preuß, *Theor. Chim. Acta*, 1990, **77**, 123–141.

9 (*a*) S. Chen, R. Rousseau, S. Raugei, M. Dupuis, D. L. DuBois and R. M. Bullock, *Organometallics*, 2011, **30**, 6108–6118; (*b*) X.-J. Qi, Y. Fu, L. Liu and Q.-X. Guo, *Organometallics*, 2007, **26**, 4197–4203; (*c*) N. Kumar and P. M. Kozlowski, *J. Phys. Chem. B*, 2013, **117**, 16044–16057; (*d*) S. Chen, M.-H. Ho, R. M. Bullock, D. L. DuBois, M. Dupuis, R. Rousseau and S. Raugei, *ACS Catal.*, 2014, **4**, 229–242; (*e*) N. Kumar, J. Kuta, W. Galezowski and P. M. Kozlowski, *Inorg. Chem.*, 2013, **52**, 1762–1771.

10 (*a*) D. E. Berning, B. C. Noll and D. L. DuBois, *J. Am. Chem. Soc.*, 1999, **121**, 11432–11447; (*b*) D. L. DuBois and D. E. Berning, *Appl. Organomet. Chem.*, 2000, **14**, 860–862; (*c*) C. J. Curtis, A. Miedaner, W. W. Ellis and D. L. DuBois, *J. Am. Chem. Soc.*, 2002, **124**, 1918–1925.

11 L. Cao, C. Sun, N. Sun, L. Meng and D. Chen, *Dalton Trans.*, 2013, **42**, 5755–5763.

12 (*a*) A. Urakawa, F. Jutz, G. Laurenczy and A. Baiker, *Chem. – Eur. J*, 2007, **13**, 3886–3899; (*b*) A. Urakawa, M. Iannuzzi, J. Hutter and A. Baiker, *Chem. – Eur. J*, 2007, **13**, 6828–6840.

